GPEN: Global Positional Encoding Network for Graphs

Anonymous authors
Paper under double-blind review

Abstract

Non-grid-structured data, *e.g.*, citation networks, social networks, and web page networks, is often represented as graphs. However, such data cannot fit into Convolutional Neural Networks (CNNs) like images because of the variable size of unordered nodes and the uncertain number of neighbours for each node. Thus, Graph Neural Networks (GNNs) have been designed. They use a message-passing scheme to aggregate each node's and its neighbours' feature representations, regardless of the number of nodes and their order. Introducing feature-independent encoding methods to GNNs is crucial to preserving graphs' structural information and making node representations more discriminative. However, local-distance-aware methods, *e.g.*, DE-GNN, only contain the information within subgraphs, resulting in ambiguity when comparing two subgraphs with the same structure. In this paper, our Global Positional Encoding Network (GPEN) is proposed to embed each node's global positional information by calculating their distances to a set of randomly sampled referential nodes. We employ contrastive loss on pairwise distances of different nodes to make positional representations more discriminative while retaining the relative interactions between nodes. We evaluate our GPEN on node classification datasets by inserting the encoding scheme into a backbone GNN and demonstrate that it outperforms state-of-the-art encoding methods on homophilic graph grains by up to 33.12% in accuracy.

1 Introduction

Graph Neural Networks (GNNs) have become famous for analyzing non-grid-structured data, like citation networks, social networks, and web page networks, which can be represented as graphs Kipf & Welling (2017); Yanardag & Vishwanathan (2015); Pei et al. (2020); Xu et al. (2019); Veličković et al. (2018); Hamilton et al. (2017). GNNs employ a message-passing scheme to recursively aggregate a central node's and neighbours' features in graphs. Specifically, node/edge representations are passed through the edges to their nearby nodes. Then, these representations are aggregated as new central node representations using permutation-invariant functions and learnable parameters. This process is repeated k times, resulting in a feature vector representing the central node, capturing the structural information and node feature distribution within the central node's k-hop neighbourhood Hamilton et al. (2017).

Although the message-passing scheme helps GNNs gather structural information based on node and edge attributes, and enables GNNs to perform well in specific domains, that ability becomes limited when applied to more diverse applications, such as forecasting passenger flow levels in airports, predicting airline connections, or classifying social networks that lack node and edge attributes Yanardag & Vishwanathan (2015); Ribeiro et al. (2017); Zhang & Chen (2018). Some strategies have been proposed to address this limitation. They rely on attribute-independent and deterministic features, such as hand-crafted rules Zhang & Chen (2018); You et al. (2021) and random-walk-based probability Li et al. (2020), to encode the distance between central nodes and their neighbours in a given locality. The goal is to learn the topological nature of graphs or subgraphs as a unique representation based on the encoded distance, which can then be used for various downstream tasks. Encoding the distance of a central-neighbour pair as a vector and combining it with the neighbour's attributes during message-passing can effectively learn local structural information. This technique has been proven to enhance the accuracy of GNNs in node classification tasks Yin et al. (2020). However, we argue that local-distance-aware encoding approaches fail to deliver discriminative features when
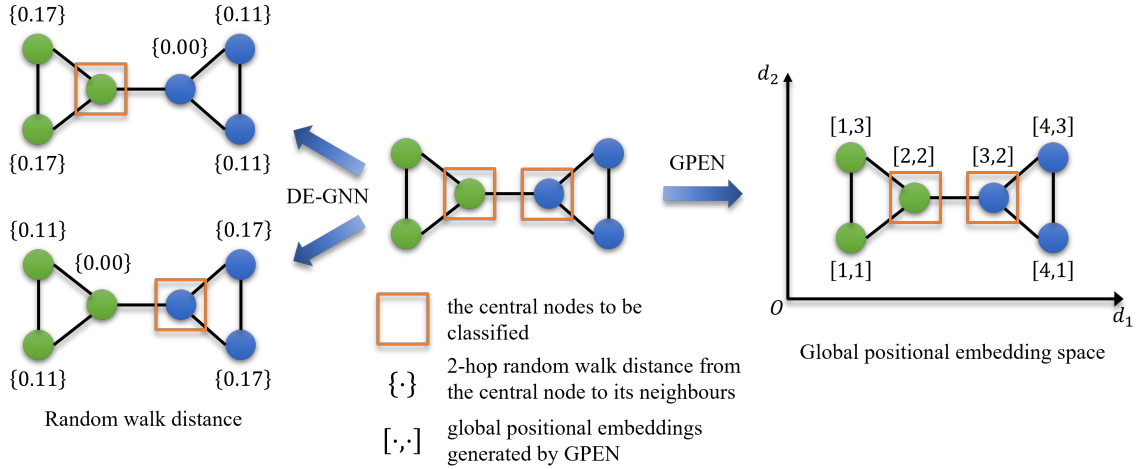
Figure 1: Intuitive comparison of DE-GNN and GPEN. **Central**: A symmetric graph where the colour of the nodes indicates their classes. **Left**: Given one central node, DE-GNN uses 2-hop random walk distance from the central node to its neighbours as node features. In this case, the encoding method generates identical features for the central nodes. **Right**: To distinguish the central nodes, GPEN generates unique global positional embeddings through contrastive learning.

two subgraphs have a similar structure but are located in different parts of the same graph, as the left part of Figure 1 shows. As a result, these non-discriminative features will harm the expressiveness of GNNs when the ground truth labels of those nodes are different. Therefore, learning the global position of each node, which contains structural information and makes similar subgraphs possible to distinguish from each other, is more important.

In this paper, we present the Global Positional Encoding Network (GPEN), which generates a distinct global positional embedding for each node in a graph based on graph structure without needing either node or edge attributes, as demonstrated in Figure 1. Unlike DE-GNN Li et al. (2020) employing relative distances between a central node and its neighbours, GPEN randomly chooses nodes from the graph as a referential node set. Each node's global position in the graph is determined by the set of vectors representing random walk probabilities between the node and the referential nodes. For each node, GPEN embeds the probability-like vectors as a positional embedding, which allows the downstream networks to learn the structure representations. We utilize self-supervised learning He et al. (2020) to ensure that the positional embeddings are consistent and able to distinguish between different nodes. We apply a contrastive loss to learn the embeddings. In this approach, we consider embeddings of the same node under different reference sets as positive pairs and aim to maximize their similarity.

In a nutshell, our contributions are summarized as follows:

1. We reveal that distance encoding approaches have limitations in providing useful graph structure information for the node classification task on homophilic graphs.

2. We propose a framework named GPEN to generate a global positional embedding for each node according to a referential node set, without needing either node or edge attributes.

3. We introduce contrastive learning to the progress of training the GPEN, which increases the stability of the global positional embedding.

We use GraphSAGE as the backbone GNN and combine it with GPEN as well as various positional or distance encoding methods. Our experiments on the node classification task have shown that GPEN significantly improves the results for datasets facing the challenges mentioned earlier. GPEN generates global positional embeddings that can effectively represent the structural information of a graph, even when node attributes are absent.

2   Related Work

GNNs. Given a central node in a graph in each layer of a GNN, the message-passing scheme generates a new node feature by aggregating features from neighbours of the central node and mapping them to a new feature space. Following this principle, many GNN designs are proposed and applied to various tasks. GCN maps features by approximating a graph convolution filter Kipf & Welling (2017). GAT applies the self-attention mechanism to the aggregation function Veličković et al. (2018). GraphSAGE concatenates central node features and aggregates neighbour features before passing them to the mapping function Hamilton et al. (2017). Regardless of the variety of aggregation and mapping functions, their corresponding computational graphs determine the final node representations containing structural information, as shown in Figure 2. Thus, the expressiveness of the GNN is limited if the computational graphs of nodes are not distinctive enough. This limitation becomes even more significant when node/edge attributes are unavailable as input.
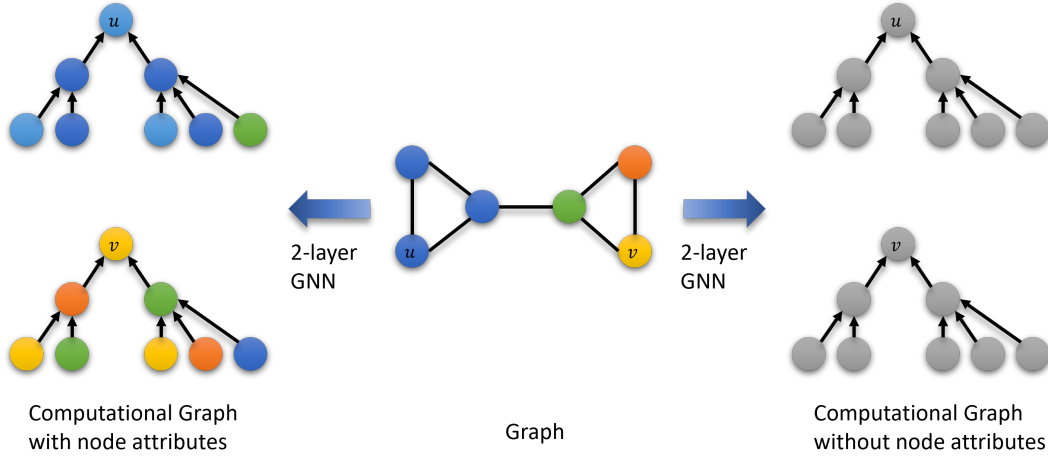

Figure 2: When passing a graph to a GNN, the computational graph shows the aggregation path of neighbours' features to the central node. **Left**: The computational graphs of the node u and v are distinctive when having node attributes. **Right**: The computational graphs of the node u and v are the same when no node attributes are available.

Distance and Positional Encoding. Introducing features independent of node/edge attributes to GNNs is a way to enhance their ability to distinguish between different instances. Two types of representations that meet this requirement are distance encoding (DE) and positional encoding (PE). Usually, GNNs learn local or global structure representations from aggregating these embeddings and then use them in node/edge/graph level tasks.

DE approaches aim to define the distances between the central node and its k-hop neighbours in subgraphs. For example, to predict the existence of a link between two target nodes, SEAL labels other nodes surrounding target nodes according to hand-crafted rules based on the shortest path distance Zhang & Chen (2018). DE-GNN encodes the distance between each node and a target node set in a subgraph using random walk probabilities Li et al. (2020). The target node set is the target of the task, such as single nodes (node classification), node pairs (link prediction), and node sets (triangle prediction). Although using positional encoding like Laplacian eigenmaps Belkin & Niyogi (2003) to generate the positional feature for each node, PEG maps the features between the end nodes to their edge as weights, which act as distances Wang et al. (2022). So, we classify PEG as a distance encoding method. These local-distance-aware methods have a common drawback: structure representations are indistinguishable in the case of similar subgraphs.

On the other hand, PE approaches lean toward a unique global positional embedding for each node, which implicitly contains structural information while making the representation diverse. Dwivedi et al. (2020) assigns a Laplacian eigenvector to each node as their positional encoding, but this method suffers from instability of multiple eigenvalues, and the computational complexity limits the application on large-scale graphs. ID-GNN colours the ego network's central node, indicating its position You et al. (2021). P-

GNN encodes each node's position in the graph into a low dimensional metric space through random walk probabilities to a randomly selected node set You et al. (2019). Following Bourgain's Theorem Bourgain (1985), this method provides a less computationally complex and relatively stable way to generate global positional representations. However, the length of P-GNN's position embeddings depends on the number of nodes, and it only uses the embeddings on edge-level tasks, which limits its capability as a general solution.

Contrastive Learning. Contrastive Learning aims to capture the invariant representation of different data augmentation He et al. (2020); Chopra et al. (2005); Chen et al. (2020); Chen & He (2021); Zhang et al. (2022), *e.g.*, low-level data augmentation of an image, while keeping the semantic meaning. Technically speaking, it pulls the positive samples closer while pushing negative samples away to achieve such invariance through optimizing the InfoNCE loss Oord et al. (2018). Since contrastive learning is independent of downstream tasks, it can be naturally applied to graph-based tasks. GCC Qiu et al. (2020) samples ego networks based on random walks to augment the graph structures for contrastive learning. MVGRL Hassani & Khasahmadi (2020) uses graph diffusion and subgraph sampling to generate different views of the same graph. GraphCL You et al. (2020) develops contrastive learning for GNN pre-training and proposes augmenting the graph through edge dropping and perturbation Rong et al. (2019). Those methods adopt the InfoNCE to find invariant feature representations via perturbing the original graph structure with different augmentation methods, failing to find a unique position representation for each node in different graph structures.
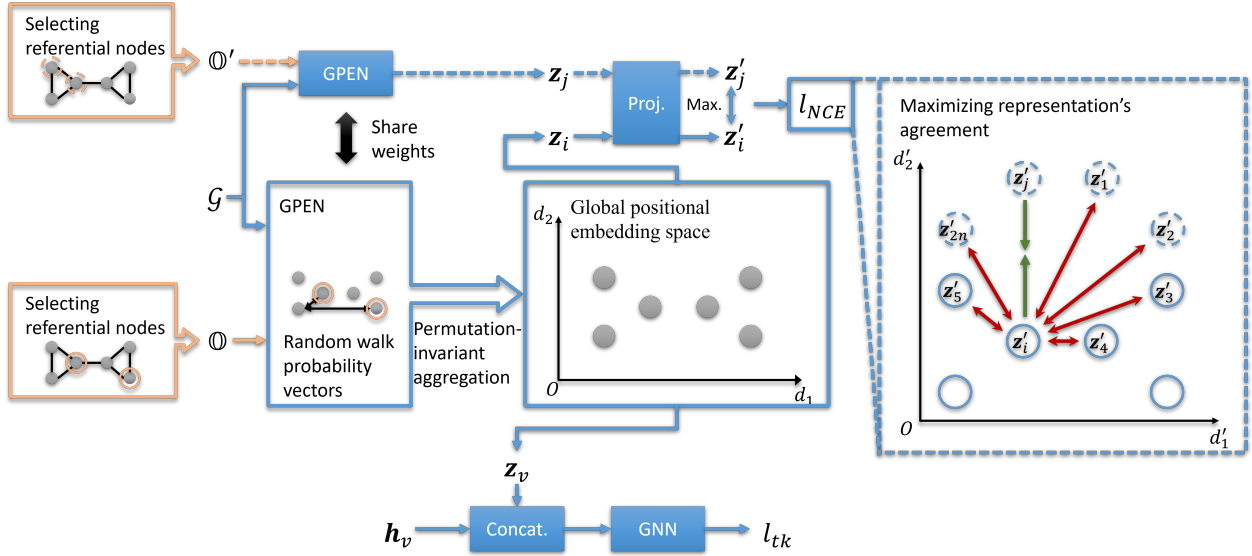
3 Method

Figure 3: The general scheme of our Global Positional Encoding Network (GPEN). Given a graph $\mathcal{G} = (\mathbb{V}, \mathbb{E})$, a referential node set $\mathbb{O} \in 2^{\mathbb{V}} \setminus \varnothing$, and a node v, GPEN uses random walk probability vectors to describe the relative distances between v and each node in the $\mathbb{O}$. Then, GPEN generates a global positional embedding z_v using a permutation-invariant aggregation function with learnable parameters. z_v can either be concatenated with the node attribute of v, h_v, or as the only input feature and sent to the backbone GNN. To keep the consistency of global positional embeddings of the same node under different selections of referential node set, GPEN generates z_i and z_j for the same node from two different referential node sets $\mathbb{O}$ and $\mathbb{O}'$, respectively. Then, we map the embeddings to a representation space as z_i' and z_j' by a nonlinear projection head and employ InfoNCE loss, aiming to maximise these representations' agreement. In this space, representations of the same node under the different referential node selections are pulled towards each other. The representations of different nodes are pushed away.

Given a graph $\mathcal{G} = (\mathbb{V}, \mathbb{E})$, where $\mathbb{V}$ is a node set and $\mathbb{E}$ is an edge set, we define a global positional embedding space. In this space, all nodes are assigned a unique position that reflects their global positions in the graph.

We propose GPEN to learn this global positional embedding space from pre-defined pair-wise node distances in the graph, which provides a more powerful encoding for describing structural information. As Figure 3 shown, GPEN generates a global position embedding for each node based on its pair-wise node distances to a randomly selected node set, which can be concatenated with the node attribute and sent to any GNN model for arbitrary tasks. Additionally, we apply a contrastive learning loss to the embeddings to ensure they are unique and consistent with each node's global position under different node set selections.

3.1 Relative Distance in Graph

Firstly, we define the distance between any two nodes in a graph to describe the local structure. The distance should be permutation-invariant because the same graph with different orders of the nodes' indices can result in different adjacency matrices.

Definition 3.1 *Given any two nodes $u, v \in \mathbb{V}$ in the graph $\mathcal{G}$, the k-step random walk probability from u to v is defined as:*

$$p^{(k)}(v|u) = (\boldsymbol{W}^k)_{uv}, \tag{1}$$

$$(\boldsymbol{W})_{uv} = \begin{cases} (\boldsymbol{A})_{uv} \big(\sum_{v=1}^{|\mathbb{V}|} (\boldsymbol{A})_{uv} \big)^{-1}, & \text{if } uv \in \mathbb{E}, \\ 0, & \text{otherwise,} \end{cases} \tag{2}$$

where $\boldsymbol{A}$ is the adjacency matrix of $\mathcal{G}$.

We add multiple random walk probabilities from node u to v with different steps to obtain more local structure information. As $\boldsymbol{W}$ can be asymmetric, we choose a vector $\boldsymbol{y}_{uv} \in \mathbb{R}^{2k}$ to describe the relative distance from node u to v in graph $\mathcal{G}$. $\boldsymbol{y}_{uv}$ consists of a sequence of k-step random walk probabilities from node u to v and v to u as:

$$\boldsymbol{y}_{uv} = \Big[p^{(1)}(v|u), ..., p^{(k)}(v|u), p^{(1)}(u|v), ..., p^{(k)}(u|v) \Big]. \tag{3}$$

3.2 Global Positional Encoding Network

However, there is still a limitation that the relative distance vector $\boldsymbol{y}_{uv}$ is insufficient to provide structural information to distinguish any two target nodes, *e.g.*, v_1 and v_2. Given two subgraphs $\mathcal{G}_1 = (\mathbb{V}_1, \mathbb{E}_1)$ and $\mathcal{G}_2 = (\mathbb{V}_2, \mathbb{E}_2)$ separately around the target node $v_1 \in \mathbb{V}_1$ and $v_2 \in \mathbb{V}_2$ in $\mathcal{G}$, where $v_1 \neq v_2$ and $\mathcal{G}_1 \neq \mathcal{G}_2$, there is a function $f : \mathbb{Y}_{uv} \to \mathbb{R}^n$ that extracts the structural information around the (u, v) pair. To achieve the permutation-invariant property, we apply a summation to aggregate the structural information and obtain the structural representation of node v:

$$h(\mathbb{Y}_{uv}) = \sum_{\boldsymbol{y} \in \mathbb{Y}_{uv}} f(\boldsymbol{y}), \tag{4}$$

where $\mathbb{Y}_{uv} = \{\boldsymbol{y}_{uv} | u \in \mathbb{V}\}$ is a multiset. When $\mathbb{Y}_{uv_1} = \{\boldsymbol{y}_{uv_1} | u \in \mathbb{V}_1\}$, $\mathbb{Y}_{uv_2} = \{\boldsymbol{y}_{uv_2} | u \in \mathbb{V}_2\}$, and $\mathbb{Y}_{uv_1} = \mathbb{Y}_{uv_2}$, A GNN cannot distinguish v_1 and v_2 by using their structural information $h(\mathbb{Y}_{uv_1})$ and $h(\mathbb{Y}_{uv_2})$ alone. This limitation will harm the representation ability when labels of v_1 and v_2 differ. Thus, we design the GPEN inspired by P-GNN You et al. (2019) to address this limitation.

Definition 3.2 *Selecting a set of nodes $\mathbb{O} = \{o_1, o_2, ..., o_{N_r}\} \in 2^{\mathbb{V}} \setminus \varnothing$, $N_r = |\mathbb{O}|$, the global position of a node $v \in \mathbb{V}$ in the graph $\mathcal{G}$ can be defined as a multiset of relative distance vectors: $\mathbb{Y}_v = \{\boldsymbol{y}_{ov} | o \in \mathbb{O}\}$. Nodes composing the set $\mathbb{O}$ are named referential nodes.*

When $\mathbb{O}$ is appropriately selected, $\mathbb{Y}_{v_1}$ can be different to $\mathbb{Y}_{v_2}$ even if $h(\mathbb{Y}_{uv_1}) = h(\mathbb{Y}_{uv_2})$. The intuition of selecting referential nodes is that each of them is sampled from the whole graph instead of a subgraph. It

serves as a coordinate axis that breaks the similarity of the local structure and can be used to encode a unique and global position for all nodes in the graph.

To encode the global position, we propose the Global Positional Encoding Network (GPEN), which generates a global positional embedding for each node:

$$\boldsymbol{z}_v = f_{GPEN}(\mathbb{Y}_v) = f_2\Big(\sum_{\boldsymbol{y} \in \mathbb{Y}_v} f_1(\boldsymbol{y})\Big), \tag{5}$$

where f_1 and f_2 are two two-layer MLPs with a non-linearity. $\boldsymbol{z}_v \in \mathbb{R}^{d_{GP}}$. d_{GP} is the dimension of the global positional embedding. Then, global positional embeddings can be individually used or concatenated with node attributes as new inputs of any GNNs. In this paper, we uniformly select N_r nodes at random in a graph as referential nodes.

3.3 Contrastive Loss

Our goal is to enable GPEN to learn unique global positional embeddings for all nodes in a graph. Using these positional embeddings, the following GNN can generate discriminative local structure representations of subgraphs in the same graph, even if they have the same structure. Meanwhile, the referential node set $\mathbb{O}$ defines the global position, which is randomly selected. Thus, maintaining consistency in the global positional embedding of the same node is essential. To achieve these two goals, P-GNN follows Bourgain's Theorem and samples almost all nodes in a graph multiple times. However, P-GNN loses the flexibility of applying the embedding to arbitrary tasks while minimizing the distortion of the positional embedding. In contrast, we only select a small number of unrepeated nodes and employ the InfoNCE loss Oord et al. (2018) to GPEN during the training stage to meet these two goals.

Inspired by SimCLR Chen et al. (2020), for each target node in the same minibatch with N samples, a projection head $f_{Proj} : \boldsymbol{z}_v \rightarrow \mathbb{R}^{d_{Proj}}$ first maps the global positional embedding to a d_{Proj}-dimensional representation space:

$$\boldsymbol{z}'_v = f_{Proj}(\boldsymbol{z}_v). \tag{6}$$

We choose a two-layer MLP with nonlinearity as the projection head in this paper. As Figure 3 shows, we separately pass the same batch of nodes with two different referential node sets, $\mathbb{O}$ and $\mathbb{O}'$, to GPEN, then acquiring projections $\boldsymbol{z}'_{\mathbb{O}}$ and $\boldsymbol{z}'_{\mathbb{O}'}$ corresponding to $\mathbb{O}$ and $\mathbb{O}'$, resulting in a set $\{\boldsymbol{z}'_k | k = 1, 2, ..., 2N\}$. Given a pair of positive samples $\boldsymbol{z}'_i, \boldsymbol{z}'_j \in \{\boldsymbol{z}'_k\}$, which are from the same node, the purpose of the contrastive prediction task is identifying $\boldsymbol{z}'_j$ in $\{\boldsymbol{z}'_k\} \setminus \{\boldsymbol{z}'_i\}$ for $\boldsymbol{z}'_i$. Therefore, the InfoNCE loss is chosen to minimize the distance of the positive pair $(\boldsymbol{z}'_i, \boldsymbol{z}'_j)$ and push other negative samples away:

$$l_{NCE} = \frac{1}{2N} \sum_{i=1}^{2N} -\log \frac{\exp\big(d(\boldsymbol{z}'_i, \boldsymbol{z}'_j)/\tau\big)}{\sum_{k=1, k \neq i}^{2N} \exp\big(d(\boldsymbol{z}'_i, \boldsymbol{z}'_k)/\tau\big)}, \tag{7}$$

$$d(\boldsymbol{z}'_i, \boldsymbol{z}'_j) = \frac{\boldsymbol{z}'_i \boldsymbol{z}'^T_j}{\|\boldsymbol{z}'_i\| \|\boldsymbol{z}'_j\|}, \tag{8}$$

where τ is a temperature parameter.

In the end, the total loss l_{tot} is formulated as:

$$l_{tot} = l_{tk} + l_{NCE}, \tag{9}$$

where l_{tk} is the loss used in the original task, *e.g.*, cross-entropy loss.

4 Experiments

4.1 Datasets

In this paper, we evaluate our models on eight public datasets for node classification tasks. All graphs are undirected and contain self-loops. The statistics of the datasets are listed in Table 1.

Citation networks. Cora and Citeseer Sen et al. (2008) are widely used citation networks where each node represents a paper, and edges denote the relationship of citations between papers. Node attributes are the bag-of-words representation of papers, and node labels are the academic topics of papers.

Wikipedia network. Chameleon and Squirrel are two page-page networks from the Wikipedia network proposed by Rozemberczki et al. (2021). Each node in the network represents a web page, and an edge represents a mutual link between two web pages. Node attributes are the presence of particular nouns on the web page, and the task is to classify the amount of average monthly traffic on each web page.

Actor co-occurrence network. Actor is a subgraph of the film-director-actor-writer network proposed by Tang et al. (2009). Nodes in the graph represent actors, and their attributes correspond to keywords in the Wikipedia pages. Edges connect nodes if actors appear on the same Wikipedia page. The target is to predict the category of each node in terms of words on their Wikipedia page.

WebKB. Cornell, Texas, and Wisconsin belong to the WebKB [1] dataset, which collects web pages from university computer science departments. Nodes in a graph represent web pages, and edges represent hyperlinks among them. Node attributes are the bag-of-words representation of web pages. The task is to predict the node label from student, project, course, staff, and faculty.

To identify properties of datasets, we introduce the metric of homophilic proposed by Pei et al. (2020):

$$\beta = \frac{1}{|\mathbb{V}|} \sum_{v \in \mathbb{V}} \frac{n_{same}}{n_{neighbor}}, \tag{10}$$

where n_{same} is the number of v's neighbors whose labels are same as v, $n_{neighbor}$ is the number of v's neighbors, and $0 \leq \beta \leq 1$. A dataset with a larger β value tends to be homophilous, meaning nodes with the same label tend to connect to each other and form a cluster. In turn, a graph with a small β value is heterophilic.

Table 1: Dataset statistics.

Dataset	Cora	Cite.	Cham.	Squi.	Actor	Corn.	Texa.	Wisc.
# Nodes	2708	3327	2277	5201	7600	183	183	251
# Edges	5429	4732	36101	217073	33544	295	309	499
# Features	1433	3703	2325	2089	931	1703	1703	1703
# Classes	7	6	5	5	5	5	5	5

4.2 Experimental Setup

To evaluate the effectiveness of our GPEN, we select various DE and PE approaches for comparison, including DE-GNN, PEG, and P-GNN. Following DE-GNN, we use a two-layer GraphSAGE as the backbone model, and its configuration is kept the same per dataset. DE and PE embeddings from GPEN, DE-GNN, and P-GNN are concatenated with node attributes along the channel dimension. Particularly, the referential node set in GPEN and the anchor-sets in P-GNN are independently sampled for each epoch as You et al. (2019) does. Meanwhile, PEG is directly built upon GraphSAGE because it essentially is an approach that uses Laplacian eigenmaps to generate edge weights for the backbone model. We conduct the experiments on all datasets in two settings: 1. with node attributes and 2. without node attributes. In the case of the setting without node attributes, we adopt the approach used in Yin et al. (2020), where the degrees of each node replace the node attributes as the input.

---

[1] http://www.cs.cmu.edu/afs/cs.cmu.edu/project/theo-11/www/wwkb/

We follow the procedure proposed by Pei et al. (2020) for all experiments. Models are trained and evaluated with ten fixed random seeds, and splits of training, validation, and test sets provided by Pei et al. (2020). The accuracy on the test set is recorded when the model achieves the highest accuracy on the validation set. All results are reported in the form of average accuracy over ten fixed splits of the test set. The Adam optimizer is adopted with $\beta_1 = 0.9$, and $\beta_2 = 0.999$. The temperature parameter τ used in InfoNCE loss is set to 1. During the training, the learning rate is reduced by a factor of two after 50 epochs with no improvement of the loss in WebKB, or ten epochs in other datasets. The training progress will stop when the learning rate is lower than $1e - 6$ or the number of epochs exceeds 500. We randomly select about $10\% - 30\%$ of the nodes across a graph with equal probabilities to form the referential node set. Other hyper-parameters are searched through grid search and selected according to the best evaluation set results. The appendix A lists the search space, all final hyper-parameters, and model architectures. The code is implemented using PyTorch Amos et al. (2018) and runs on an Nvidia Tesla V100 16GB GPU.

4.3 Results and Analysis

Table 2: Accuracy (%) of state-of-the-art and GPEN augmented models on datasets whose $\beta \geq 0.22$. **Bold**: the best results. <u>Underline</u>: the second-best results.

Type	Dataset β Attr.	Cora 0.83 w/	w/o	Cite. 0.71 w/	w/o	Cham. 0.25 w/	w/o	Squi. 0.22 w/	w/o	Actor 0.24 w/	w/o
None	GraphSAGE	83.58	38.67	**75.25**	33.4	61.23	51.51	40.07	37.23	36.57	**25.49**
DE	DE-GNN	<u>84.41</u>	41.51	74.17	32.31	<u>61.78</u>	44.21	<u>41.55</u>	38.83	<u>36.86</u>	25.27
	PEG	83.90	38.23	73.98	32.63	61.03	<u>52.35</u>	41.10	<u>41.32</u>	**36.90**	25.36
PE	P-GNN	83.86	<u>48.47</u>	73.61	<u>48.33</u>	49.41	49.91	37.27	39.73	35.63	<u>25.48</u>
	GPEN	**86.16**	**71.35**	<u>74.63</u>	**49.81**	**68.95**	**66.80**	**48.27**	**51.81**	36.63	24.91

Table 3: Accuracy (%) of state-of-the-art and GPEN augmented models on datasets whose $\beta < 0.22$. **Bold**: the best results. <u>Underline</u>: the second-best results.

Type	Dataset β Attr.	Corn. 0.11 w/	w/o	Texa. 0.06 w/	w/o	Wisc. 0.16 w/	w/o
None	GraphSAGE	75.14	<u>58.92</u>	78.92	**72.43**	<u>82.75</u>	55.49
DE	DE-GNN	74.05	58.65	76.22	66.76	80.00	**57.84**
	PEG	**80.00**	**59.19**	**80.81**	63.51	**85.29**	<u>55.69</u>
PE	P-GNN	<u>75.95</u>	58.92	<u>79.46</u>	<u>70.27</u>	79.41	54.51
	GPEN	71.62	55.95	76.76	69.73	78.24	**57.84**

We evaluate GPEN and other state-of-the-art encoding methods in scenarios where node attributes are available or absent. We generally find that PE methods, especially GPEN, outperform DE methods on graphs tending to be homophilous. Thus, we roughly divide the results into Table 2 and 3 for datasets with $\beta \geq 0.22$ and $\beta < 0.22$, respectively.

When $\beta \geq 0.22$, DE methods can barely achieve similar results to the GraphSAGE backbone model. However, as a PE method, P-GNN has notable accuracy on Cora and Citeseer when the node attributes are absent. It struggles to provide meaningful positional information to supplement node features when $\beta < 0.71$. On the contrary, GPEN has almost the highest accuracy on Cora, Citeseer, Chameleon, and Squirrel. It exceeds P-GNN by up to 19.54% on Chameleon when using node attributes. If removing the node attributes, GPEN even surpasses the accuracy of PEG by 33.12% on Cora. Furthermore, when comparing the results of using node attributes on Squirrel, GPEN increases its accuracy by 3.54% after removing the node attributes.

We show the limitations of GPEN that it fails on datasets with $\beta < 0.22$, where PEG outperforms other models. The intuitive explanation is that nodes with the same label cluster in datasets with high β values. PE methods preserve these clusters by mapping the graph's structure to a global positional embedding space, resulting in more distinguishable embeddings for nodes from different clusters. On the other hand, DE

methods generate similar features when the subgraphs' structure between different clusters is alike, making it difficult to distinguish between them. When the β value decreases, nodes in a graph start reflecting their roles. For instance, in the WebKB dataset, nodes with the same role have similar local structures surrounding them, and vice versa. Although these nodes may be distributed anywhere in the graph, they possess specific roles. Consequently, introducing explicit local structure representations with DE methods may perform better than PE methods.

4.4 Ablation Study

4.4.1 Visualization of Global Positional Embeddings

To support our explanation in Sec. 4.3, we generate global positional embeddings using GPEN on various graphs and visualize them in two-dimensional space through t-SNE Van der Maaten & Hinton (2008). To exclude the influence of node attributes, we use GPEN trained without them. We observed that the embeddings are more distinguishable on graphs with larger β values, as shown in Figure 4. On Cora and Chameleon, the embeddings form distinct clusters for different classes. However, GPEN fails to provide distinguishable embeddings on Actor and Cornell, as nodes from different classes are evenly distributed in the embedding space.
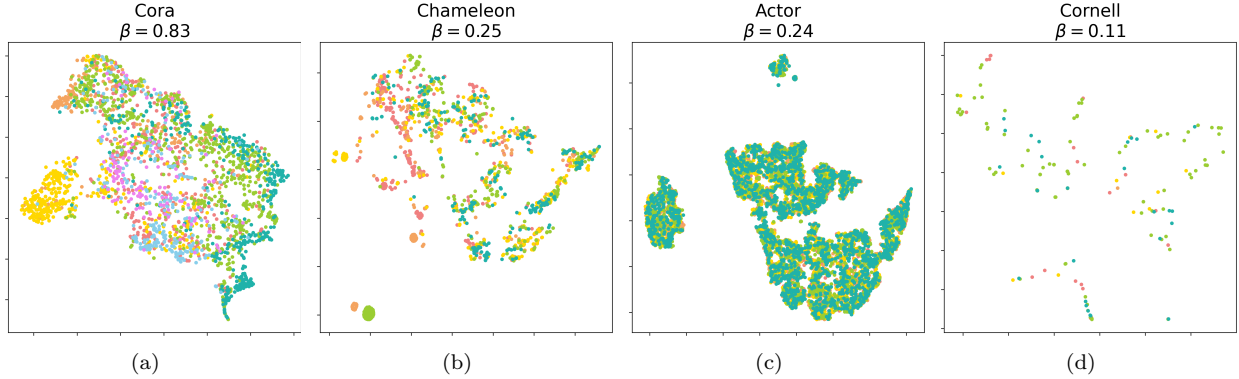

Figure 4: Visualization of global positional embeddings generated by GPEN through t-SNE. The colour of points represents the class of nodes.

4.4.2 Stability of Global Positional Embeddings

It is essential to examine the stability of the global positional embeddings generated by GPEN when the referential nodes change, as they are randomly selected. Therefore, we evaluate the stability of pre-trained GPEN, and GPEN without using InfoNCE loss (GPEN-w/o-l_{NCE}) on all datasets. We randomly select the referential nodes 1,000 times for each test set split. We calculate the average standard deviations (s.d.) of the accuracy for each split to obtain the s.d. result of the dataset, as shown in Table 4 and 5.

Table 4: Ablation study on stability of global positional embeddings. Models are trained on datasets whose $\beta \geq 0.22$. The standard deviations (s.d.) of accuracy (%) are compared in parallel. A lower s.d. is better. ↑: higher s.d. of GPEN after using the InfoNCE loss. ↓: lower s.d. of GPEN after using the InfoNCE loss.

Dataset	Cora		Cite.		Cham.		Squi.		Actor	
Attr.	w/	w/o	w/	w/o	w/	w/o	w/	w/o	w/	w/o
GPEN-w/o-l_{NCE} (Ours)	0.749	10.919	0.270	1.669	0.834	0.880	1.046	1.227	0.245	0.209
GPEN (Ours)	↓ 0.361	↓ 7.832	↓ 0.257	↑ 1.888	↓ 0.829	↓ 0.833	↓ 0.916	↓ 1.090	↓ 0.243	↑ 0.248

According to the findings, GPEN has relatively low s.d. compared to the accuracy on most datasets with $\beta \geq 0.22$. Meanwhile, using the InfoNCE loss on most datasets helps enhance GPEN's stability, highlighting

Table 5: Ablation study on stability of global positional embeddings. Models are trained on datasets whose $\beta < 0.22$. The standard deviations (s.d.) of accuracy (%) are compared in parallel. A lower s.d. is better. ↑: higher s.d. of GPEN after using the InfoNCE loss. ↓: lower s.d. of GPEN after using the InfoNCE loss.

Dataset	Corn.		Texa.		Wisc.	
Attr.	w/	w/o	w/	w/o	w/	w/o
GPEN-w/o-l_{NCE} (Ours)	2.619	3.096	3.439	3.462	1.636	3.560
GPEN (Ours)	↓ 1.922	↓ 1.685	↓ 2.272	↑ 5.272	↓ 1.477	↓ 3.208

the importance of incorporating contrastive learning techniques. Compared to the P-GNN sampling anchor-set based on the Bourgain theorem Bourgain (1985), our philosophy is to trade off the sampling complexity to achieve flexibility while maintaining higher accuracy by a notable margin using a simple sampling strategy and contrastive learning.

4.4.3 Transfer learning of GPEN

We conduct transfer learning experiments to test GPEN's ability to learn graph structure knowledge. We load and freeze the weights of GPEN pre-trained on the source dataset and only train the backbone model with cross-entropy loss without using node attributes on the target dataset from scratch. We denote such model as GPEN-*source dataset*. Here, we select Cora and Squirrel as the source or target dataset. Table 6 shows that although GPEN's performance is downgraded after being transferred to the new domain, it can still outperform P-GNN. The results suggest that GPEN can generalize the graph structure knowledge and potentially become a general model if trained on various graphs on a large scale.

Table 6: Ablation study of transfer learning of GPEN. Models are trained without using node attributes. Accuracy (%) is compared in parallel.

Dataset	Transfer learning	Cora	Squi.
P-GNN	✗	50.02	34.94
GPEN (Ours)		71.35	51.81
GPEN-*Squi.* (Ours)	✓	60.08	-
GPEN-*Cora* (Ours)		-	46.53

4.4.4 Relative Distance of Global Positional Embeddings

Section 4.3 suggests that DE methods, particularly PEG, perform better when dealing with Actor and WebKB datasets with small values of β. PEG creates edge weights using the L2 distance of Laplacian eigenmaps. This method is compatible with any other global positional embeddings. It is easy to test the effectiveness of embeddings from GPEN by sending them to PEG. The model, PEG-GPEN, has been trained on the previously mentioned datasets. According to the results in Table 7, PEG-GPEN achieves higher accuracy than using GPEN directly in low β value graphs. As a result, the relative distances of global positional embeddings generated by GPEN have a similar performance as Laplacian eigenmaps. This experiment shows that GPEN has an advantage in that its global positional embeddings can be easily extended to low β value graphs when using their relative distance.

Table 7: Influence of applying the relative distance of global positional embeddings generated by GPEN to PEG (PEG-GPEN). Models are trained on datasets with small β. and compared with accuracy (%). **Bold**: the best model. ↑: higher accuracy compared to GPEN. ↓: lower accuracy compared to GPEN.

Dataset	Actor		Corn.		Texa.		Wisc.	
Attr.	w/	w/o	w/	w/o	w/	w/o	w/	w/o
PEG	**36.90**	**25.36**	**80.00**	**59.19**	80.81	63.51	**85.29**	55.69
PEG-GPEN	↑ 36.82	↑ 25.07	↑ 75.95	↑ 58.65	↑ **81.08**	↓ **64.86**	↑ 82.55	↓ **55.88**

5 Conclusion and limitation

We have proposed GPEN, which generates global positional embeddings for all nodes in a graph without needing either node or edge attributes. This enhances discrimination with a relatively high degree of consistency. Our experiments have demonstrated that our global position is superior in representing structural information compared to DE methods on homophilic graphs. Our GPEN can be integrated with any GNN approach to effectively enhance their performance, particularly on node classification tasks on homophilous graphs without node attributes. We demonstrate the potential of GPEN to be independently trained on various graph structures to learn more general global positional embeddings, which can then be applied to multiple tasks. Although directly using the global positional embeddings generated by GPEN as node features on heterophilic graphs may harm the GNN, it is still possible that combining GPEN with local-distance-aware methods can make the GNN take advantage of the embeddings in such circumstances. However, universal ways of applying the embeddings to all kinds of graphs need to be explored in the future.

References

Brandon Amos, Ivan Jimenez, Jacob Sacks, Byron Boots, and J. Zico Kolter. Differentiable MPC for End-to-end Planning and Control. In *Advances in Neural Information Processing Systems*, volume 31, pp. 8289–8300, 2018.

Mikhail Belkin and Partha Niyogi. Laplacian eigenmaps for dimensionality reduction and data representation. *Neural Computation*, 15(6):1373–1396, 2003.

Jean Bourgain. On lipschitz embedding of finite metric spaces in hilbert space. *Israel Journal of Mathematics*, 52:46–52, 1985.

Ting Chen, Simon Kornblith, Mohammad Norouzi, and Geoffrey Hinton. A simple framework for contrastive learning of visual representations. In *Proceedings of the 37th International Conference on Machine Learning*, volume 119 of *Proceedings of Machine Learning Research*, pp. 1597–1607. PMLR, 13–18 Jul 2020.

Xinlei Chen and Kaiming He. Exploring simple siamese representation learning. In *Proceedings of the IEEE/CVF Conference on Computer Vision and Pattern Recognition*, pp. 15750–15758, 2021.

S. Chopra, R. Hadsell, and Y. LeCun. Learning a similarity metric discriminatively, with application to face verification. In *2005 IEEE Computer Society Conference on Computer Vision and Pattern Recognition (CVPR'05)*, volume 1, pp. 539–546 vol. 1, 2005. doi: 10.1109/CVPR.2005.202.

Vijay Prakash Dwivedi, Chaitanya K Joshi, Thomas Laurent, Yoshua Bengio, and Xavier Bresson. Benchmarking graph neural networks. *arXiv preprint arXiv:2003.00982*, 2020.

Will Hamilton, Zhitao Ying, and Jure Leskovec. Inductive Representation Learning on Large Graphs. In *Advances in Neural Information Processing Systems*, 2017.

Kaveh Hassani and Amir Hosein Khasahmadi. Contrastive multi-view representation learning on graphs. In *Proceedings of the 37th International Conference on Machine Learning*, ICML'20. JMLR.org, 2020.

Kaiming He, Haoqi Fan, Yuxin Wu, Saining Xie, and Ross Girshick. Momentum contrast for unsupervised visual representation learning. In *Proceedings of the IEEE/CVF Conference on Computer Vision and Pattern Recognition*, pp. 9729–9738, 2020.

Thomas N. Kipf and Max Welling. Semi-Supervised Classification with Graph Convolutional Networks. In *5th International Conference on Learning Representations, ICLR 2017*. OpenReview.net, 2017.

Pan Li, Yanbang Wang, Hongwei Wang, and Jure Leskovec. Distance encoding: Design provably more powerful neural networks for graph representation learning. In *Advances in Neural Information Processing Systems*, volume 33, pp. 4465–4478, 2020.

Aaron van den Oord, Yazhe Li, and Oriol Vinyals. Representation learning with contrastive predictive coding. *arXiv preprint arXiv:1807.03748*, 2018.

Hongbin Pei, Bingzhe Wei, Kevin Chen-Chuan Chang, Yu Lei, and Bo Yang. Geom-gcn: Geometric graph convolutional networks. In *International Conference on Learning Representations*, 2020.

Jiezhong Qiu, Qibin Chen, Yuxiao Dong, Jing Zhang, Hongxia Yang, Ming Ding, Kuansan Wang, and Jie Tang. Gcc: Graph contrastive coding for graph neural network pre-training. In *Proceedings of the 26th ACM SIGKDD International Conference on Knowledge Discovery & Data Mining*, KDD '20, pp. 1150–1160. Association for Computing Machinery, 2020.

Leonardo F.R. Ribeiro, Pedro H.P. Saverese, and Daniel R. Figueiredo. Struc2vec: Learning node representations from structural identity. In *Proceedings of the 23rd ACM SIGKDD International Conference on Knowledge Discovery and Data Mining*, KDD '17, pp. 385–394. Association for Computing Machinery, 2017.

Yu Rong, Wenbing Huang, Tingyang Xu, and Junzhou Huang. Dropedge: Towards deep graph convolutional networks on node classification. *arXiv preprint arXiv:1907.10903*, 2019.

Benedek Rozemberczki, Carl Allen, and Rik Sarkar. Multi-Scale attributed node embedding. *Journal of Complex Networks*, 9(2), 05 2021.

Prithviraj Sen, Galileo Namata, Mustafa Bilgic, Lise Getoor, Brian Galligher, and Tina Eliassi-Rad. Collective classification in network data. *AI Magazine*, 29(3):93, Sep. 2008.

Jie Tang, Jimeng Sun, Chi Wang, and Zi Yang. Social influence analysis in large-scale networks. In *Proceedings of the 15th ACM SIGKDD International Conference on Knowledge Discovery and Data Mining*, KDD '09, pp. 807–816. Association for Computing Machinery, 2009.

Laurens Van der Maaten and Geoffrey Hinton. Visualizing data using t-sne. *Journal of machine learning research*, 9(11), 2008.

Petar Veličković, Guillem Cucurull, Arantxa Casanova, Adriana Romero, Pietro Liò, and Yoshua Bengio. Graph attention networks. In *International Conference on Learning Representations*, 2018.

Haorui Wang, Haoteng Yin, Muhan Zhang, and Pan Li. Equivariant and stable positional encoding for more powerful graph neural networks. In *International Conference on Learning Representations*, 2022.

Minjie Wang, Da Zheng, Zihao Ye, Quan Gan, Mufei Li, Xiang Song, Jinjing Zhou, Chao Ma, Lingfan Yu, Yu Gai, Tianjun Xiao, Tong He, George Karypis, Jinyang Li, and Zheng Zhang. Deep graph library: A graph-centric, highly-performant package for graph neural networks. *arXiv preprint arXiv:1909.01315*, 2019.

Keyulu Xu, Weihua Hu, Jure Leskovec, and Stefanie Jegelka. How Powerful are Graph Neural Networks? In *International Conference on Learning Representations*, 2019.

Pinar Yanardag and S.V.N. Vishwanathan. Deep Graph Kernels. In *Proceedings of the 21th ACM SIGKDD International Conference on Knowledge Discovery and Data Mining*, KDD '15, pp. 1365–1374, 2015. doi: 10.1145/2783258.2783417. URL https://doi.org/10.1145/2783258.2783417.

Haoteng Yin, Yanbang Wang, and Pan Li. Revisiting graph neural networks and distance encoding from a practical view. *arXiv preprint arXiv:2011.12228*, 2020.

Jiaxuan You, Rex Ying, and Jure Leskovec. Position-aware graph neural networks. In *Proceedings of the 36th International Conference on Machine Learning, ICML 2019, 9-15 June 2019, Long Beach, California, USA*, volume 97 of *Proceedings of Machine Learning Research*, pp. 7134–7143, 2019.

Jiaxuan You, Jonathan M Gomes-Selman, Rex Ying, and Jure Leskovec. Identity-aware graph neural networks. *Proceedings of the AAAI Conference on Artificial Intelligence*, 35(12):10737–10745, May 2021.

Yuning You, Tianlong Chen, Yongduo Sui, Ting Chen, Zhangyang Wang, and Yang Shen. Graph contrastive learning with augmentations. *Advances in Neural Information Processing Systems*, 33:5812–5823, 2020.

Muhan Zhang and Yixin Chen. Link prediction based on graph neural networks. In *Proceedings of the 32nd International Conference on Neural Information Processing Systems*, NIPS'18, pp. 5171–5181. Curran Associates Inc., 2018.

Tong Zhang, Congpei Qiu, Wei Ke, Sabine Süsstrunk, and Mathieu Salzmann. Leverage your local and global representations: A new self-supervised learning strategy. *arXiv preprint arXiv:2203.17205*, 2022.

A Appendix

A.1 Code

Our code[2] is implemented using PyTorch Amos et al. (2018), DGL Wang et al. (2019), and following projects:

1. Benchmarking Graph Neural Networks[3] Dwivedi et al. (2020);

2. Geo-GCN[4] Pei et al. (2020);

3. DE-GNN[5] Yin et al. (2020);

4. PEG[6] Wang et al. (2022);

5. P-GNN[7] You et al. (2019);

6. SimCLR[8] Chen et al. (2020).

A.2 Architecture Details

The details of the models used in this paper are illustrated in the following section.

A.2.1 GraphSAGE Backbone

The GraphSAGE Hamilton et al. (2017) module in the *l*-th layer of GraphSAGE backbone is formulated as:

$$h_v^{l+1} = \text{ReLU}\big(U\,\text{Concat}(h_v^l, \text{Mean}_{u\in\mathcal{N}(v)}h_u^l)\big),\tag{11}$$

where $U \in \mathbb{R}^{d_{out}\times 2d_{in}}$, $\mathcal{N}(v)$ is the neighbours of the central node v. The architecture of the GraphSAGE backbone used for the node classification task in this paper is illustrated in Fig. 5.

Figure 5: Architecture of the GraphSAGE backbone. h_v: the node attribute of the central node v. $\{h_{\mathcal{N}(v)}\}$ the node attribute set of the central node v's neighbours. d_{in}: the dimension of inputs. d_{hid}: the dimension of hidden layers. d_{class}: the number of classes. $U_{class1} \in \mathbb{R}^{d_{hid}\times d_{hid}}$. $U_{class2} \in \mathbb{R}^{d_{class}\times d_{hid}}$.

---

[2]The source code is available at `https://github.com/Anonymous/GPEN`
[3]`https://github.com/graphdeeplearning/benchmarking-gnns`
[4]`https://github.com/graphdml-uiuc-jlu/geom-gcn`
[5]`https://github.com/VeritasYin/DEGNN_node_classification`
[6]`https://github.com/Graph-COM/PEG`
[7]`https://github.com/RecLusIve-F/P-GNN-dgl`
[8]`https://github.com/Spijkervet/SimCLR`

A.2.2 DE-GNN

The DE-GNN Li et al. (2020) generates a distance embedding for each node pair using k-hop random walk distance. Given a central node v and a node u, the embedding $\boldsymbol{l}_{uv} \in \mathbb{R}^k$ is formulated as:

$$\boldsymbol{l}_{uv} = [(\boldsymbol{W})_{uv}, (\boldsymbol{W}^2)_{uv}, ..., (\boldsymbol{W}^k)_{uv}], \tag{12}$$

where $(\boldsymbol{W}^k)_{uv}$ is the k-step random walk probability from the node u to v. The architecture of the DE-GNN with the GraphSAGE backbone used for the node classification task in this paper is illustrated in Fig. 6.
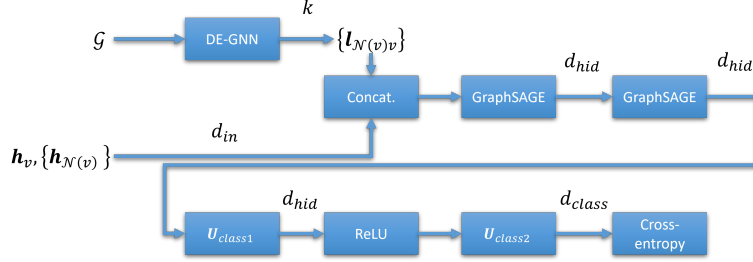

Figure 6: Architecture of the DE-GNN combined with the GrapSAGE backbone. $\mathcal{G}$: the input graph. $\boldsymbol{h}_v$: the node attribute of the central node v. $\{\boldsymbol{h}_{\mathcal{N}(v)}\}$ the node attribute set of the central node v's neighbours. d_{in}: the dimension of inputs. k: the number of hops of random walk. $\{\boldsymbol{l}_{\mathcal{N}(v)v}\}$: the set of distance embeddings from the central node v's neighbours to the v. d_{hid}: the dimension of hidden layers. d_{class}: the number of classes. $\boldsymbol{U}_{class1} \in \mathbb{R}^{d_{hid} \times d_{hid}}$. $\boldsymbol{U}_{class2} \in \mathbb{R}^{d_{class} \times d_{hid}}$.

A.2.3 PEG

The PEG Wang et al. (2022) aims to generate a stable edge weight using Laplacian eigenmaps:

$$\xi_{uv} = \sigma\big(\boldsymbol{U}_2 \boldsymbol{U}_1 \, \|\boldsymbol{z}_u - \boldsymbol{z}_v\|\big), \tag{13}$$

where $\boldsymbol{z}_u$ and $\boldsymbol{z}_v$ are p smallest eigenvectors of the node u and v, respectively. $\boldsymbol{U}_1^T, \boldsymbol{U}_2 \in \mathbb{R}^{d_{hid_e}}$.

When combining the PEG with the GraphSAGE module, Eq. 11 is re-formulated as:

$$\boldsymbol{h}_v^{l+1} = \text{ReLU}\Big(\boldsymbol{U}\text{Concat}\big(\boldsymbol{h}_v^l, \text{Mean}_{u \in \mathcal{N}(v)}(\xi_{uv}\boldsymbol{h}_u^l)\big)\Big). \tag{14}$$

The architecture of the PEG combined with the GraphSAGE backbone used for the node classification task in this paper is illustrated in Fig. 7.

Figure 7: Architecture of the PEG combined with the GraphSAGE backbone. $\boldsymbol{h}_v$: the node attribute of the central node v. $\{\boldsymbol{h}_{\mathcal{N}(v)}\}$ the node attribute set of the central node v's neighbours. $\boldsymbol{z}_{\mathcal{N}}(v)$: p smallest eigenvectors of the central node v's neighbours. $\boldsymbol{z}_v$: p smallest eigenvectors of the central node v. $\{\xi_{\mathcal{N}(v)v}\}$: the set of edge weights between the central node v's neighbours and the v. d_{in}: the dimension of inputs. d_{hid}: the dimension of hidden layers. d_{class}: the number of classes. $\boldsymbol{U}_{class1} \in \mathbb{R}^{d_{hid} \times d_{hid}}$. $\boldsymbol{U}_{class2} \in \mathbb{R}^{d_{class} \times d_{hid}}$.

A.2.4 P-GNN

Given any two nodes v and u in a graph $\mathcal{G} = (\mathbb{V}, \mathbb{E})$, P-GNN You et al. (2019) first defines their distance in the $\mathcal{G}$:

$$s(v, u) = \frac{1}{d_{sp}^q(v, u) + 1}, \tag{15}$$

$$d_{sp}^q(v, u) = \begin{cases} d_{sp}(v, u), & \text{if } d_{sp}(v, u) \leq q, \\ \infty, & \text{otherwise}, \end{cases} \tag{16}$$

where $d_{sp}(v, u)$ is the shortest path between v and u. q is the longest searching hop which should be no larger than the diameter of $\mathcal{G}$.

Following the Bourgain theorem Bourgain (1985), P-GNN samples anchor-sets $\mathbb{S}_{i,j} \subset \mathbb{V}, i = 1, 2, ..., \lceil \log n \rceil, j = 1, 2, ..., \lceil \log n \rceil, n = |\mathbb{V}|$. The total number of anchor-sets is $N_{\mathbb{S}} = \lceil \log n \rceil^2$. For each anchor-set $\mathbb{S}_{i,j}$, P-GNN independently sample each node from $\mathbb{V}$ with probability $\frac{1}{2^i}$.

For each node $v \in \mathbb{V}$ in the l-th layer of the P-GNN module, a matrix $\boldsymbol{M}^l \in \mathbb{R}^{d_{hid} \times N_{\mathbb{S}}}$ of anchor-set messages is generated based on anchor-sets. Each column of $\boldsymbol{M}^l$ is an anchor-set message $\boldsymbol{M}_i^l$ formulated as:

$$\boldsymbol{M}_i^l = \text{ReLU}\big(s(v, u)\boldsymbol{U}_1^l \text{Concat}(\boldsymbol{h}_v^l, \boldsymbol{h}_u^l)\big), \forall u \in \underset{u \in \mathbb{S}_{i,j}}{\arg\min} \, d(v, u), i = 1, 2, ..., \lceil \log n \rceil, j = 1, 2, ..., \lceil \log n \rceil, \tag{17}$$

where $\boldsymbol{U}_1^l \in \mathbb{R}^{d_{out} \times 2d_{in}}$. Then, we can obtain the position-aware embedding $\boldsymbol{z}_v^l$ and the message $\boldsymbol{h}_v^{l+1}$ for the node v:

$$\boldsymbol{z}_v^l = \boldsymbol{U}_2^l \boldsymbol{M}^l, \tag{18}$$

$$\boldsymbol{h}_v^{l+1} = \text{Mean}_{i \in \{1, 2, ..., N_{\mathbb{S}}\}} \boldsymbol{M}_i^l, \tag{19}$$

where $\boldsymbol{U}_2^l \in \mathbb{R}^{d_{out}}$.

Following the original paper, we use two layers of the P-GNN module. The architecture of the P-GNN combined with the GraphSAGE backbone used for the node classification task in this paper is illustrated in Fig. 8.
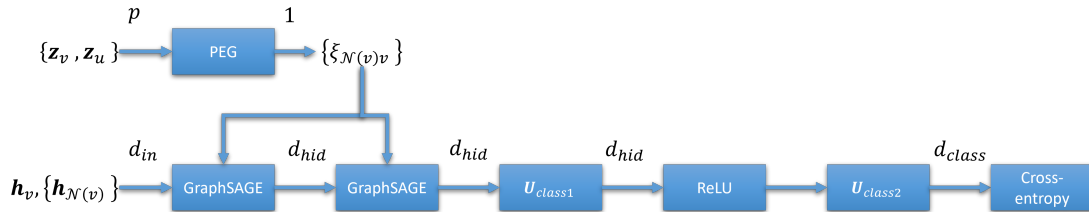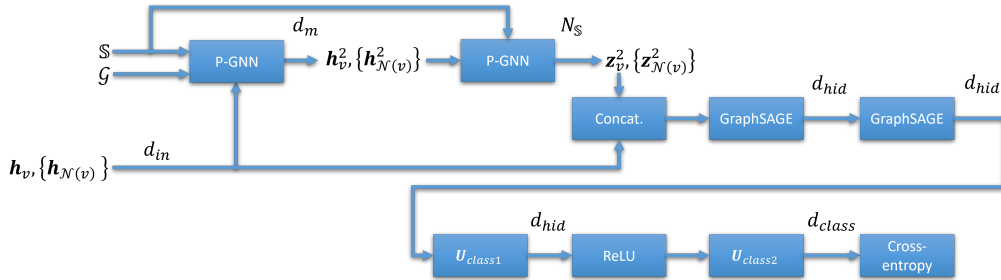

Figure 8: Architecture of the P-GNN combined with the GraphSAGE backbone. $\boldsymbol{h}_v$: the node attribute of the central node v. $\{\boldsymbol{h}_{\mathcal{N}(v)}\}$ the node attribute set of the central node v's neighbours. $\boldsymbol{h}_v^2$: the second layer input message of the central node v. $\boldsymbol{h}_{\mathcal{N}}^2(v)$: the set of the second layer input messages of the central node v's neighbours. d_m: the dimension of the messages. $\boldsymbol{z}_v^2$: the second layer output position-aware embedding of the node v. $\{\boldsymbol{z}_{\mathcal{N}}^2(v)\}$: the set of the second layer output position-aware embeddings of the central node v's neighbours. d_{in}: the dimension of inputs. d_m: the dimension of output messages in the P-GNN. $N_{\mathbb{S}}$: the total number of anchor-sets. d_{hid}: the dimension of hidden layers. d_{class}: the number of classes. $\boldsymbol{U}_{class1} \in \mathbb{R}^{d_{hid} \times d_{hid}}$. $\boldsymbol{U}_{class2} \in \mathbb{R}^{d_{class} \times d_{hid}}$.

A.2.5 GPEN

As Fig. 9 shows, our GPEN consists of two two-layer MLPs and summation aggregation to generate the global positional embeddings for each node. Fig. 10 illustrates the projection head that maps the global positional

embeddings to a representation space where the InfoNCE loss Oord et al. (2018) trains the GPEN. The architecture of the GPEN combined with the GraphSAGE backbone used for the node classification task in this paper is shown in Fig. 11.
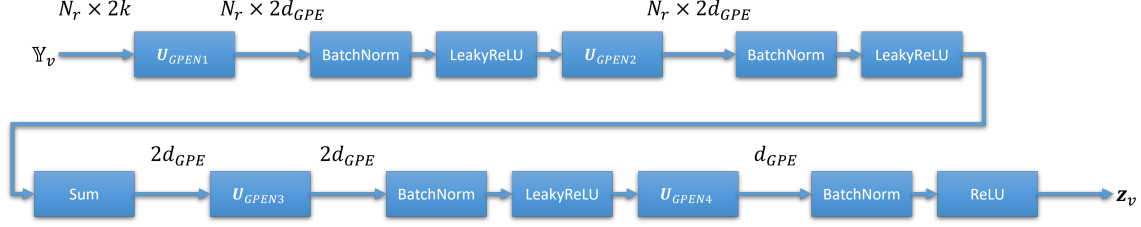

Figure 9: Architecture of the GPEN. k: the number of steps of random walk. $\mathbb{Y}_v$: The k-step random walk probability vector set representing distances from referential nodes to node v. N_r: the number of referential nodes. d_{GPE}: the dimension of the global positional embedding. $\boldsymbol{z}_v$: the global positional embedding of the node v. $\boldsymbol{U}_{GPEN1} \in \mathbb{R}^{2k \times 2d_{GPE}}$. $\boldsymbol{U}_{GPEN2}, \boldsymbol{U}_{GPEN3} \in \mathbb{R}^{2d_{GPE} \times 2d_{GPE}}$. $\boldsymbol{U}_{GPEN4} \in \mathbb{R}^{2d_{GPE} \times d_{GPE}}$
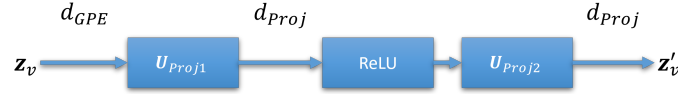
Figure 10: Architecture of projection head. $\boldsymbol{z}_v$: the global positional embedding of the node v. d_{GPE}: the dimension of the global positional embedding. d_{Proj}: the output dimension of the projection head. $\boldsymbol{z}'_v$: the projection of the node v's global positional embedding. $\boldsymbol{U}_{Proj1} \in \mathbb{R}^{d_{GPE} \times d_{Proj}}$. $\boldsymbol{U}_{Proj2} \in \mathbb{R}^{d_{Proj} \times d_{Proj}}$.
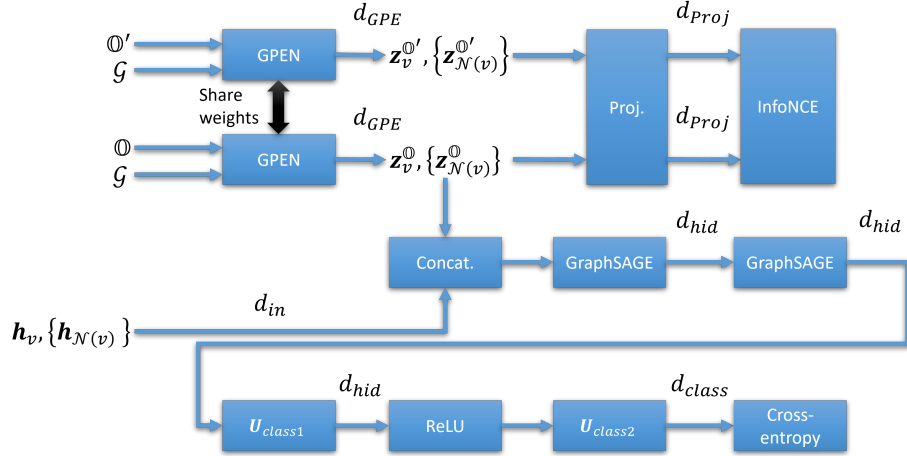
Figure 11: Architecture of the GPEN combined with the GrapSAGE backbone. $\mathbb{O}, \mathbb{O}'$: the referential node sets with different node selections. $\mathcal{G}$: the input graph. $\boldsymbol{h}_v$: the node attribute of the central node v. $\{\boldsymbol{h}_{\mathcal{N}(v)}\}$ the node attribute set of the central node v's neighbours. d_{in}: the dimension of inputs. d_{GPE}: the dimension of the global positional embedding. $\boldsymbol{z}_v^{\mathbb{O}}, \boldsymbol{z}_v^{\mathbb{O}'}$: the global positional embedding of the node v under the corresponding referential node set. $\{\boldsymbol{z}_{\mathcal{N}}^{\mathbb{O}}(v)\}, \{\boldsymbol{z}_{\mathcal{N}}^{\mathbb{O}'}(v)\}$: the set of the global positional embeddings of the central node v's neighbours under the corresponding referential node set. d_{Proj}: the output dimension of the projection head. d_{hid}: the dimension of hidden layers. d_{class}: the number of classes. $\boldsymbol{U}_{class1} \in \mathbb{R}^{d_{hid} \times d_{hid}}$. $\boldsymbol{U}_{class2} \in \mathbb{R}^{d_{class} \times d_{hid}}$.

A.2.6 PEG-GPEN

We replace the eigenvectors used in PEG with the global positional embeddings generated by GPEN and name the architecture PEG-GPEN. The design of PEG-GPEN combined with the GraphSAGE backbone is illustrated in Fig. 12.
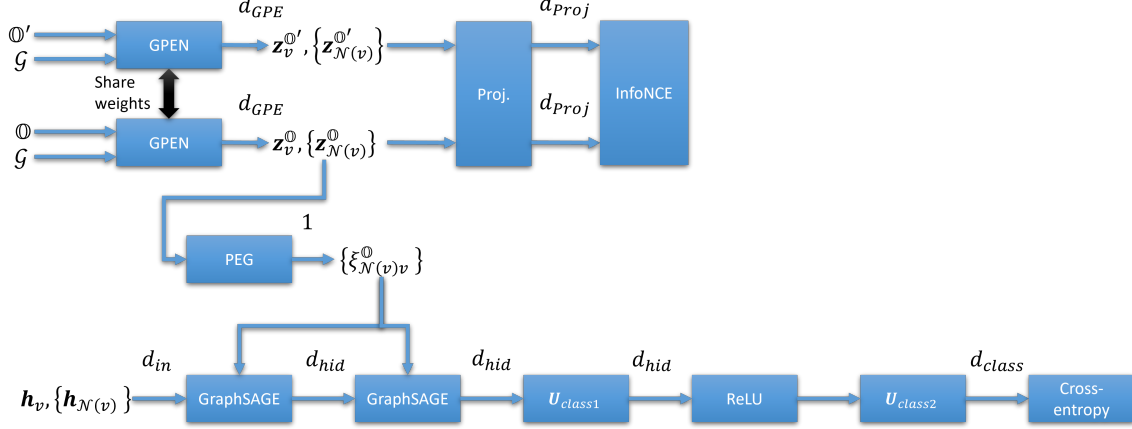
Figure 12: Architecture of the PEG combined with the GrapSAGE backbone using the global positional embeddings generated by the GPEN. $\mathbb{O}$, $\mathbb{O}'$: the referential node sets with different node selections. $\mathcal{G}$: the input graph. $\boldsymbol{h}_v$: the node attribute of the central node v. $\{\boldsymbol{h}_{\mathcal{N}(v)}\}$ the node attribute set of the central node v's neighbours. d_{in}: the dimension of inputs. d_{GPE}: the dimension of the global positional embedding. $\boldsymbol{z}_v^{\mathbb{O}}$, $\boldsymbol{z}_v^{\mathbb{O}'}$: the global positional embedding of the node v under the corresponding referential node set. $\{\boldsymbol{z}_{\mathcal{N}}^{\mathbb{O}}(v)\}$, $\{\boldsymbol{z}_{\mathcal{N}}^{\mathbb{O}'}(v)\}$: the set of the global positional embeddings of the central node v's neighbours under the corresponding referential node set. $\{\xi_{\mathcal{N}(v)v}^{\mathbb{O}}\}$: the set of edge weights between the central node v's neighbours and the v under the corresponding referential node set. d_{Proj}: the output dimension of the projection head. d_{hid}: the dimension of hidden layers. d_{class}: the number of classes. $\boldsymbol{U}_{class1} \in \mathbb{R}^{d_{hid} \times d_{hid}}$. $\boldsymbol{U}_{class2} \in \mathbb{R}^{d_{class} \times d_{hid}}$.

A.3 Hyper-parameter Details

The hyper-parameter search space of all experiments conducted by ourselves is listed as Table 8. After the grid search, we select the final hyper-parameters for each experiment according to its best validation set result. The final hyper-parameters of each experiment are listed as Table 9, 10, 11, 12, 13, 14, 15, 16, 17, 18, 19, 20, 21, 22, 23, and 24.

Table 8: Hyper-parameter search space of all experiments conducted by ourselves. wd: weight decay. $drop$: dropout rate. k: the number of steps of random walk. N_r factor: percentage of referential nodes compared to total nodes in a graph. lr_{init}: initial learning rate.

Hyperparameter	Search space	Dataset
wd	1e-6, 5e-5	
$drop$	0.2, 0.4	All
k	5, 10, 20	
Nr factor	10%, 20%, 30%	Cora, Cite., Cham., Corn., Texa., Wisc.
	10%, 15%	Actor
	10%, 20%	Squi.
lr_{init}	1e-3, 5e-3, 1e-2	Corn., Texa., Wisc.
	1e-4, 5e-4, 1e-3	Cham., Squi.
	5e-4, 1e-3, 5e-3	Cora, Cite., Actor

Table 9: Final hyper-parameters of the GraphSAGE using node attributes. lr_{init}: initial learning rate. wd: weight decay. bs: batch size. $drop$: dropout rate. d_{hid}: the number of hidden units.

Dataset	Cora	Cite.	Cham.	Squi.	Actor	Corn.	Texa.	Wisc.
lr_{init}	5e-3	1e-3	1e-3	1e-3	5e-4	5e-3	1e-2	1e-2
wd	1e-6	1e-6	1e-6	1e-6	1e-6	5e-5	5e-5	5e-5
bs	32	32	32	8	16	16	16	16
$drop$	0.4	0.4	0.2	0.2	0.4	0.4	0.4	0.4
d_{hid}	32	32	64	32	32	64	64	64

Table 10: Final hyper-parameters of the GraphSAGE without using node attributes. lr_{init}: initial learning rate. wd: weight decay. bs: batch size. $drop$: dropout rate. d_{hid}: the number of hidden units.

Dataset	Cora	Cite.	Cham.	Squi.	Actor	Corn.	Texa.	Wisc.
lr_{init}	5e-3	5e-3	1e-3	1e-3	1e-3	1e-3	5e-3	1e-2
wd	1e-6	1e-6	1e-6	1e-6	1e-6	5e-5	5e-5	5e-5
bs	32	32	32	8	16	16	16	16
$drop$	0.4	0.4	0.2	0.2	0.4	0.4	0.4	0.4
d_{hid}	32	32	64	32	32	64	64	64

Table 11: Final hyper-parameters of the DE-GNN combined with the GrapSAGE backbone using node attributes. lr_{init}: initial learning rate. wd: weight decay. bs: batch size. $drop$: dropout rate. k: the number of steps of random walk. d_{hid}: the number of hidden units.

Dataset	Cora	Cite.	Cham.	Squi.	Actor	Corn.	Texa.	Wisc.
lr_{init}	5e-3	1e-3	5e-4	1e-3	5e-4	1e-2	5e-3	5e-3
wd	1e-6	1e-6	1e-6	1e-6	1e-6	5e-5	5e-5	5e-5
bs	32	32	32	8	16	16	16	16
$drop$	0.4	0.4	0.2	0.2	0.4	0.4	0.4	0.4
k	10	5	5	20	20	10	5	5
d_{hid}	32	32	64	32	32	64	64	64

Table 12: Final hyper-parameters of the DE-GNN combined with the GrapSAGE backbone without using node attributes. lr_{init}: initial learning rate. wd: weight decay. bs: batch size. $drop$: dropout rate. k: the number of steps of random walk. d_{hid}: the number of hidden units.

Dataset	Cora	Cite.	Cham.	Squi.	Actor	Corn.	Texa.	Wisc.
lr_{init}	5e-3	1e-3	1e-3	1e-3	5e-4	1e-3	1e-2	1e-2
wd	1e-6	1e-6	1e-6	1e-6	1e-6	5e-5	5e-5	5e-5
bs	32	32	32	8	16	16	16	16
$drop$	0.4	0.4	0.2	0.2	0.4	0.4	0.4	0.4
k	5	10	20	5	5	5	10	10
d_{hid}	32	32	64	32	32	64	64	64

Table 13: Final hyper-parameters of the PEG combined with the GrapSAGE backbone using node attributes. lr_{init}: initial learning rate. wd: weight decay. bs: batch size. $drop$: dropout rate. p smallest eigenvectors. d_{hid_e}: the number of hidden units in PEG. d_{hid}: the number of hidden units in other parts of the model.

Dataset	Cora	Cite.	Cham.	Squi.	Actor	Corn.	Texa.	Wisc.
lr_{init}	5e-3	5e-4	5e-4	1e-3	1e-3	1e-2	1e-2	1e-2
wd	1e-6	1e-6	1e-6	1e-6	1e-6	5e-5	5e-5	5e-5
bs	32	32	32	8	16	16	16	16
$drop$	0.4	0.4	0.2	0.2	0.4	0.4	0.4	0.4
p	128	128	128	128	128	128	128	128
d_{hid_e}	32	32	32	32	32	32	32	32
d_{hid}	32	32	64	32	32	64	64	64

Table 14: Final hyper-parameters of the PEG combined with the GrapSAGE backbone without using node attributes. lr_{init}: initial learning rate. wd: weight decay. bs: batch size. $drop$: dropout rate. p: p smallest eigenvectors. d_{hid_e}: the number of hidden units in PEG. d_{hid}: the number of hidden units in other parts of the model.

Dataset	Cora	Cite.	Cham.	Squi.	Actor	Corn.	Texa.	Wisc.
lr_{init}	5e-3	5e-3	1e-3	1e-3	5e-3	5e-3	1e-2	1e-2
wd	1e-6	1e-6	1e-6	1e-6	1e-6	5e-5	5e-5	5e-5
bs	32	32	32	8	16	16	16	16
$drop$	0.4	0.4	0.2	0.2	0.4	0.4	0.4	0.4
p	128	128	128	128	128	128	128	128
d_{hid_e}	32	32	32	32	32	32	32	32
d_{hid}	32	32	64	32	32	64	64	64

Table 15: Final hyper-parameters of the P-GNN combined with the GrapSAGE backbone using node attributes. lr_{init}: initial learning rate. wd: weight decay. bs: batch size. $drop$: dropout rate. d_m: the dimension of output messages in the P-GNN. d_{hid}: the number of hidden units.

Dataset	Cora	Cite.	Cham.	Squi.	Actor	Corn.	Texa.	Wisc.
lr_{init}	5e-3	5e-3	1e-3	1e-3	5e-4	1e-2	1e-2	1e-2
wd	1e-6	1e-6	1e-6	1e-6	1e-6	5e-5	5e-5	5e-5
bs	32	32	32	8	16	16	16	16
$drop$	0.4	0.4	0.2	0.2	0.4	0.4	0.4	0.4
d_m	32	32	64	32	32	64	64	64
d_{hid}	32	32	64	32	32	64	64	64

Table 16: Final hyper-parameters of the P-GNN combined with the GrapSAGE backbone without using node attributes. lr_{init}: initial learning rate. wd: weight decay. bs: batch size. $drop$: dropout rate. d_m: the dimension of output messages in the P-GNN. d_{hid}: the number of hidden units.

Dataset	Cora	Cite.	Cham.	Squi.	Actor	Corn.	Texa.	Wisc.
lr_{init}	5e-3	5e-3	5e-4	1e-3	5e-4	1e-3	1e-3	1e-3
wd	1e-6	1e-6	1e-6	1e-6	1e-6	5e-5	5e-5	5e-5
bs	32	32	32	8	16	16	16	16
$drop$	0.4	0.4	0.2	0.2	0.4	0.4	0.4	0.4
d_m	32	32	64	32	32	64	64	64
d_{hid}	32	32	64	32	32	64	64	64

Table 17: Final hyper-parameters of the GPEN combined with the GrapSAGE backbone using node attributes. N_r factor: percentage of referential nodes compared to total nodes in a graph. lr_{init}: initial learning rate. wd: weight decay. bs: batch size. $drop$: dropout rate. k: the number of steps of random walk. d_{GPE}: the dimension of the global positional embeddings. d_{hid}: the number of hidden units. d_{Proj}: the output dimension of the projection head.

Dataset	Cora	Cite.	Cham.	Squi.	Actor	Corn.	Texa.	Wisc.
N_r factor	10%	30%	20%	20%	10%	10%	10%	20%
lr_{init}	1e-3	1e-3	5e-4	1e-4	1e-3	1e-3	1e-2	1e-2
wd	1e-6	1e-6	1e-6	1e-6	1e-6	5e-5	5e-5	5e-5
bs	32	32	32	8	16	16	16	16
$drop$	0.4	0.4	0.2	0.2	0.4	0.4	0.4	0.4
k	5	10	5	10	20	5	5	10
d_{GPE}	32	32	64	32	32	64	64	64
d_{hid}	32	32	64	32	32	64	64	64
d_{Proj}	32	32	64	32	32	64	64	64

Table 18: Final hyper-parameters of the GPEN combined with the GrapSAGE backbone without using node attributes. N_r factor: percentage of referential nodes compared to total nodes in a graph. lr_{init}: initial learning rate. wd: weight decay. bs: batch size. $drop$: dropout rate. k: the number of steps of random walk. d_{GPE}: the dimension of the global positional embeddings. d_{hid}: the number of hidden units. d_{Proj}: the output dimension of the projection head.

Dataset	Cora	Cite.	Cham.	Squi.	Actor	Corn.	Texa.	Wisc.
N_r factor	30%	20%	30%	20%	15%	30%	10%	20%
lr_{init}	5e-3	5e-3	1e-3	1e-3	1e-3	1e-4	1e-3	1e-3
wd	1e-6	1e-6	1e-6	1e-6	1e-6	5e-5	5e-5	5e-5
bs	32	32	32	8	16	16	16	16
$drop$	0.4	0.4	0.2	0.2	0.4	0.4	0.4	0.4
k	20	10	20	5	10	5	5	20
d_{GPE}	32	32	64	32	32	64	64	64
d_{hid}	32	32	64	32	32	64	64	64
d_{Proj}	32	32	64	32	32	64	64	64

Table 19: Final hyper-parameters of the GPEN combined with the GrapSAGE backbone using node attributes and without using InfoNCE loss. N_r factor: percentage of referential nodes compared to total nodes in a graph. lr_{init}: initial learning rate. wd: weight decay. bs: batch size. $drop$: dropout rate. k: the number of steps of random walk. d_{GPE}: the dimension of the global positional embedding. d_{hid}: the number of hidden units. d_{Proj}: the output dimension of the projection head.

Dataset	Cora	Cite.	Cham.	Squi.	Actor	Corn.	Texa.	Wisc.
N_r factor	20%	20%	30%	20%	10%	10%	10%	10%
lr_{init}	5e-4	5e-4	5e-4	1e-4	1e-3	5e-3	5e-3	5e-3
wd	1e-6	1e-6	1e-6	1e-6	1e-6	5e-5	5e-5	5e-5
bs	32	32	32	8	16	16	16	16
$drop$	0.4	0.4	0.2	0.2	0.4	0.4	0.4	0.4
k	20	10	5	5	5	5	5	20
d_{GPE}	32	32	64	32	32	64	64	64
d_{hid}	32	32	64	32	32	64	64	64
d_{Proj}	32	32	64	32	32	64	64	64

Table 20: Final hyper-parameters of the GPEN combined with the GrapSAGE backbone without using node attributes and InfoNCE loss. N_r factor: percentage of referential nodes compared to total nodes in a graph. lr_{init}: initial learning rate. wd: weight decay. bs: batch size. $drop$: dropout rate. k: the number of steps of random walk. d_{GPE}: the dimension of the global positional embedding. d_{hid}: the number of hidden units. d_{Proj}: the output dimension of the projection head.

Dataset	Cora	Cite.	Cham.	Squi.	Actor	Corn.	Texa.	Wisc.
N_r factor	20%	30%	30%	20%	10%	10%	30%	20%
lr_{init}	5e-3	5e-3	1e-3	5e-4	1e-3	1e-2	5e-3	1e-2
wd	1e-6	1e-6	1e-6	1e-6	1e-6	5e-5	5e-5	5e-5
bs	32	32	32	8	16	16	16	16
$drop$	0.4	0.4	0.2	0.2	0.4	0.4	0.4	0.4
k	20	10	10	10	20	20	10	10
d_{GPE}	32	32	64	32	32	64	64	64
d_{hid}	32	32	64	32	32	64	64	64
d_{Proj}	32	32	64	32	32	64	64	64

Table 21: Final hyper-parameters of the PEG-GPEN combined with the GrapSAGE backbone using node attributes. N_r factor: percentage of referential nodes compared to total nodes in a graph. lr_{init}: initial learning rate. wd: weight decay. bs: batch size. $drop$: dropout rate. k: the number of steps of random walk. d_{GPE}: the dimension of the global positional embedding. d_{hid_e}: the number of hidden units in PEG. d_{hid}: the number of hidden units in other parts of the model. d_{Proj}: the output dimension of the projection head.

Dataset	Actor	Corn.	Texa.	Wisc.
N_r factor	10%	20%	20%	10%
lr_{init}	1e-3	1e-3	1e-2	5e-3
wd	1e-6	5e-5	5e-5	5e-5
bs	16	16	16	16
$drop$	0.4	0.4	0.4	0.4
k	5	5	10	20
d_{GPE}	32	64	64	64
d_{hid_e}	32	32	32	32
d_{hid}	32	64	64	64
d_{Proj}	32	64	64	64

Table 22: Final hyper-parameters of the PEG-GPEN combined with the GrapSAGE backbone without using node attributes. N_r factor: percentage of referential nodes compared to total nodes in a graph. lr_{init}: initial learning rate. wd: weight decay. bs: batch size. $drop$: dropout rate. k: the number of steps of random walk. d_{GPE}: the dimension of the global positional embedding. d_{hid_e}: the number of hidden units in PEG. d_{hid}: the number of hidden units in other parts of the model. d_{Proj}: the output dimension of the projection head.

Dataset	Actor	Corn.	Texa.	Wisc.
N_r factor	15%	20%	20%	10%
lr_{init}	5e-4	1e-3	1e-2	1e-2
wd	1e-6	5e-5	5e-5	5e-5
bs	16	16	16	16
$drop$	0.4	0.4	0.4	0.4
k	20	10	5	10
d_{GPE}	32	64	64	64
d_{hid_e}	32	32	32	32
d_{hid}	32	64	64	64
d_{Proj}	32	64	64	64

Table 23: Final hyper-parameters of the pre-trained GPEN combined with the GrapSAGE backbone without using node attributes. The weights of GPEN are pre-trained on Squirrel and frozen. The GraphSAGE backbone is trained on Cora only using cross-entropy loss. N_r factor: percentage of referential nodes compared to total nodes in a graph. lr_{init}: initial learning rate. wd: weight decay. bs: batch size. $drop$: dropout rate. k: the number of steps of random walk. d_{GPE}: the dimension of the global positional embedding. d_{hid}: the number of hidden units.

Dataset	Cora
N_r factor	30%
lr_{init}	5e-3
wd	1e-6
bs	32
$drop$	0.4
k	5
d_{GPE}	32
d_{hid}	32

Table 24: Final hyper-parameters of pre-trained GPEN combined with the GraphSAGE backbone without using node attributes. The weights of GPEN are pre-trained on Cora and frozen. The GraphSAGE backbone is trained on Squirrel only using cross-entropy loss. N_r factor: percentage of referential nodes compared to total nodes in a graph. lr_{init}: initial learning rate. wd: weight decay. bs: batch size. $drop$: dropout rate. k: the number of steps of random walk. d_{GPE}: the dimension of the global positional embedding. d_{hid}: the number of hidden units.

Dataset	Squi.
N_r factor	20%
lr_{init}	1e-3
wd	1e-6
bs	32
$drop$	0.4
k	20
d_{GPE}	32
d_{hid}	32